



**CHALMERS**  
UNIVERSITY OF TECHNOLOGY

---



# **Photo-induced optimization of carrier concentration for thermoelectric materials**

GUNNAR ÖRN SÍMONARSON

**PHOTO-INDUCED OPTIMIZATION OF CARRIER  
CONCENTRATION FOR THERMOELECTRIC MATERIALS**

GUNNAR ÖRN SÍMONARSON

Department of Chemical and Biological Engineering  
CHALMERS UNIVERSITY OF TECHNOLOGY  
Göteborg, Sweden 2014

Photo-induced optimization of carrier concentration for thermoelectric materials

GUNNAR ÖRN SÍMONARSON

© Gunnar Örn Símonarson, 2014.

Department of Chemical and Biological Engineering  
Chalmers University of Technology  
SE-412 96 Göteborg  
Sweden  
Telephone +46 (0) 31-772 1000

Cover: Single crystal  $\text{TiO}_2$  rutile sample illuminated by 385 nm LED lamp via optical fiber.

Printed by:  
Chalmers Reproservice  
Göteborg, Sweden 2014

## **Abstract**

Enormous amounts of heat energy are wasted in automotive exhaust and industrial processes and harvesting a part of that energy is of high interest. Thermoelectric (TE) materials, typically semi-conductors, can be utilized in a device that converts heat to electrical power through a thermal gradient. The properties that characterize the TE efficiency; electrical conductivity, thermal conductivity and the Seebeck coefficient, are affected by the charge carrier concentration in a material. These properties are interrelated and to optimize the thermoelectric performance of a material they must be compromised. One way of doing that is to control the carrier concentration. The carrier concentration is typically tuned with chemical substitution, a method which requires synthesis of a series of materials with different doping concentration. Another way is to apply electromagnetic radiation, where the carrier concentration in a material can in principle be tuned with photon flux.

The impact of light illumination on the carrier concentration and the TE properties of selected semi-conductors was investigated. Measurements of the electrical resistivity, the Seebeck coefficient and Hall effect measurement, which yield the carrier concentration, were conducted in dark and under illumination. Experimental configurations were designed to provide light illumination while performing these measurements.

The electromagnetic radiation had a great impact on the carrier concentration of titanium dioxide ( $\text{TiO}_2$ ) rutile, which is a wide band gap semi-conductor, while it did not have a measurable effect on silicon and magnesium silicide, which both have much smaller band gap. A switch from n- to p-type conduction was observed on the  $\text{TiO}_2$  sample, where at low intensities the free electron concentration decreased and after the switch to p-type conduction the hole concentration increased. A mechanism for this transition and the carrier concentration change was proposed. The light illumination had some effect on the TE properties of the materials, however there was no clear trend observed with varying light intensities.

The method of using electromagnetic radiation to find the optimum carrier concentration for TE materials may be useful for thin films, or where the light absorption layer has a measurable contribution to the bulk values of the TE properties and the carrier concentration. There might also be limitations with regards to band gap and band structure of the material.

**Keywords:** Carrier concentration, Thermoelectric, Photo-Induced

## Table of Contents

1. Introduction .....	1
1.1 Thermoelectric properties .....	2
1.2 Purpose of this study .....	2
2. Theoretical background.....	3
2.1 Thermoelectrics.....	3
2.2 Carrier concentration.....	4
2.3 Photoconductivity .....	5
2.4 Hall effect.....	7
3. Materials and methods .....	8
3.1 Thermoelectric measurements .....	8
3.2 Hall effect measurements.....	9
4. Results and discussion.....	11
4.1 Magnesium silicide .....	11
4.2 Silicon .....	12
4.3 Titanium dioxide rutile .....	14
4.4 Carrier concentration and TE properties .....	17
5. Conclusion.....	19
Acknowledgements .....	20
References .....	21
Appendix .....	23



## 1. Introduction

Thermoelectric devices can be used to convert heat to electricity and electrical power to a thermal gradient. Thermoelectric generators have been used with success in applications where reliability and durability of energy conversion is more important than the efficiency and cost, but since the early 1990's there has been development of nanostructured materials with better thermoelectric properties opening up a wider range of potential applications. That includes various industrial processes that waste tremendous amounts of heat energy, such as in a car combustion engine.

The thermoelectric effect was first described by Tomas Seebeck in a series of articles in the 1820's [1-4]. He discovered that when two different metals are electrically connected in series and thermally in parallel are exposed to a temperature gradient a deflection of an adjacent compass needle is noticed. He believed this to be a magnetic phenomenon but now it is understood that the temperature difference generates an electrical potential and the magnetic effect he observed was due to electrical current driven by that potential. The buildup of electrical potential driven by a temperature difference is therefore known as the Seebeck effect.

Jean C. Peltier reported that a temperature change is observed at the junction of two different conductive materials when an electric current is passed through it [5]. In 1838 Lenz demonstrated that depending on the current direction the junction can either be heated or cooled. He placed a water droplet onto the junction of bismuth and antimony and saw that the droplet froze when a current was applied in one direction and melted again when the current was reversed [6]. Heating or cooling at junctions caused by electrical current is known as the Peltier effect.

In 1851 William Thomson, later known as Lord Kelvin, realized and defined the relationship between the Seebeck and Peltier effect and proposed, and later observed experimentally, a new thermoelectric effect which describes the heating or cooling in a homogenous conductor when a current passes through a temperature gradient [7]. 60 years passed until Altenkirch described the properties that a good thermoelectric material should possess. That included large Seebeck coefficient, low thermal conductivity and high electrical conductivity [8, 9].

Important steps in understanding thermoelectric materials were taken in the 1950s when the use of heavily doped semiconductors became accepted. The field did not receive much attention by the scientific community in the years from 1960-1990 but applications in space missions, laboratory equipment and medical application kept the industry growing. In the early 1990s, the research community was encouraged by the US Department of Defense to consider the potential of thermoelectric materials as a contender for efficient cooling or power conversion applications. This encouragement was successful and has lead scientists in the field to new and interesting directions in developing the next generation of thermoelectric materials, including new families of advanced bulk thermoelectric materials and using low-dimensional materials systems [10].

## **1.1 Thermoelectric properties**

The performance of a thermoelectric material is characterized by a dimensionless figure-of-merit which is composed of the thermoelectric properties, the Seebeck coefficient, electrical and thermal conductivity. These properties are further discussed in chapter 2.1. The thermoelectric properties are interrelated and compromises between the properties are needed to produce a good thermoelectric material. The carrier concentration in a material has a great impact on the thermoelectric properties and one way of maximizing the efficiency of a thermoelectric material is tuning the carrier concentration. [11] That is conventionally done with chemical substitution, a method that requires synthesis of multiple materials. Another approach is to utilize electromagnetic radiation to generate electron – hole pairs, i.e. charge carriers. The amount of charge carriers can in principle be tuned by varying the intensity of light with energy higher than the band gap of the material. Conducting TE measurements on a material while it is exposed to light of varying intensities may therefore be a way to optimize the carrier concentration [12].

## **1.2 Purpose of this study**

The aim of this study is to investigate the impact of electromagnetic radiation on the carrier concentration and the TE properties of selected semi-conductors.

## 2. Theoretical background

The carrier concentration has a great impact on the thermoelectric properties of a material. The electronic transport properties were analyzed with Hall effect measurements and the Seebeck coefficient and the electrical resistivity were measured simultaneously while a temperature gradient was applied to the material.

### 2.1 Thermoelectrics

When a material is exposed to a thermal gradient, an electric potential is created and a phenomena called the thermoelectric effect can be observed. This effect is utilized in thermoelectric generators (TEG) and in Peltier coolers, where thermal energy is converted to electrical current and electrical power converted to a thermal gradient, respectively. Most modern TE devices use p-n semi-conductor junctions between hot and cold heat exchanger plates, an example of a single thermocouple is shown in Fig 2.1. A working TEG device would contain a number of these thermocouples, where the materials are connected electrically in series but thermally in parallel.

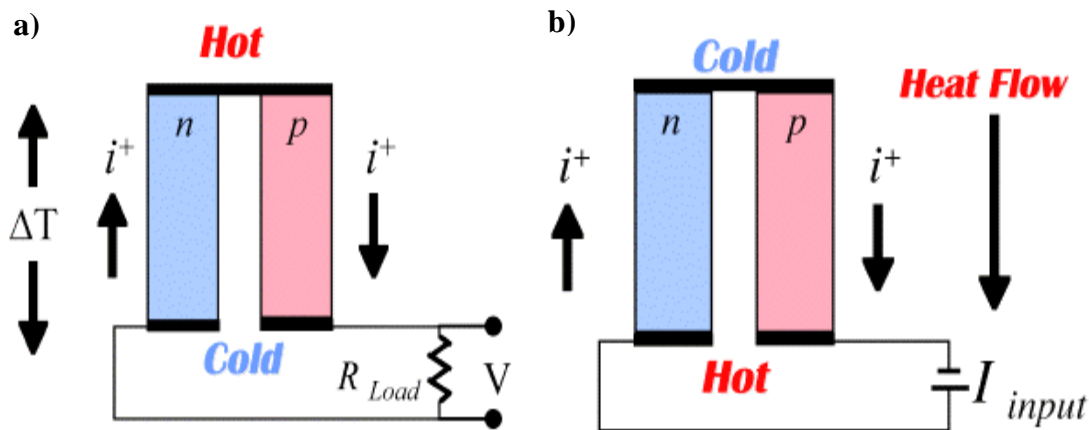


Fig 2.1 Thermocouples as used in a) power generation and b) refrigeration. [13]

The performance of TE materials is characterized by the dimensionless figure-of-merit

$$zT = \frac{\alpha^2 \sigma}{\kappa} T \quad (1)$$

where  $\alpha$  is the Seebeck coefficient,  $\sigma$  is the electrical conductivity,  $\kappa$  is the thermal conductivity and  $T$  is the absolute temperature. A material with high TE efficiency will achieve a high figure-of-merit. As equation (1) shows, a large absolute Seebeck coefficient, high electrical conductivity and low thermal conductivity is required to accomplish that. These requirements are difficult to fulfill since materials with high Seebeck coefficient tend to have low electrical conductivity and increasing electrical conductivity results in the increasing electronic contribution to the thermal conductivity.

### 2.1.1 Seebeck effect

A thermal gradient in a material will cause the electron density to be different on the cold side compared to the hot side. That difference in electron density will cause a potential difference to develop in the material. The voltage difference is quantified by the Seebeck coefficient, which is given with equation (2).

$$\alpha = -\frac{\Delta V}{\Delta T} \quad (2)$$

In p-type materials the Seebeck coefficient has a positive value, but for a n-type material the coefficient is negative. This difference is resolved in the expression for the figure-of-merit since the Seebeck coefficient is squared. Commonly  $S$  is used as a symbol for the Seebeck coefficient and in the literature the term thermopower is sometimes used for the Seebeck coefficient.

### 2.2 Carrier concentration

Finding a way to increase the thermoelectric efficiency of a material means working with properties that are related to each other and improving one usually has negative effect on another. As previously mentioned, the carrier concentration in a material has a great impact on the thermoelectric properties. Low carrier concentration results in high Seebeck coefficient and thermal conductivity, which is good in terms of thermoelectric properties; however that consequently results in low electrical conductivity. The relationship between the Seebeck coefficient and carrier concentration can be expressed as [11]

$$\alpha = \frac{8\pi^2 k_B^2}{3eh^2} m^* T \left(\frac{\pi}{3n}\right)^{\frac{2}{3}} \quad (3)$$

where  $k_B$  is the Boltzman constant,  $e$  is the charge of an electron,  $h$  is the Planck constant,  $n$  is the carrier concentration and  $m^*$  is the effective mass of the carrier. There should be only one type of charge carrier present in the material, since mixed charges will cancel out each other and the Seebeck effect in the material.

The electrical conductivity is related to the carrier concentration as shown in equation (4)

$$\sigma = \frac{1}{\rho} = ne\mu \quad (4)$$

where  $\rho$  is the electrical resistivity and  $\mu$  is the carrier mobility. The thermal conductivity has contribution from electrons ( $\kappa_{el}$ ) and phonons ( $\kappa_L$ ), an increase in carrier concentration also gives rise to the electronic contribution of the thermal conduction.

The impact of the carrier concentration on the Seebeck coefficient and the electrical conductivity are shown in Fig 2.1. The figure is not drawn directly from equations 2 and 3 but based on empirical data of thermoelectric materials. The optimal carrier concentration with regards to TE properties in a narrow band-gap semiconductor is usually between  $10^{19}$  and  $10^{21}$   $\text{cm}^{-3}$  depending on the material.

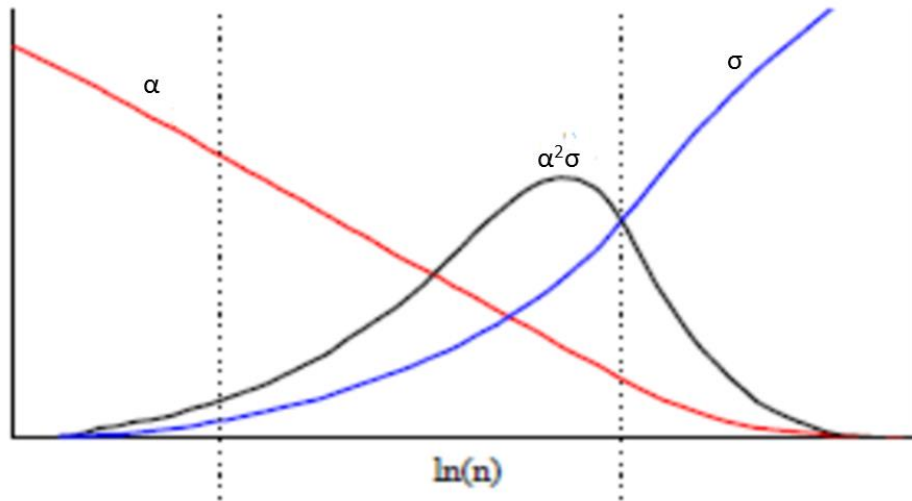


**Fig 2.2** The impact of carrier concentration on the Seebeck coefficient and the electrical conductivity. Image redrawn from [14].

### 2.3 Photoconductivity

The effect of photons increasing the electrical conductivity of a material, semi-conductors in particular, is known as photoconductivity. The conductivity is usually increased in proportion to the photon flux. There are two main types of optical absorption that may occur depending on the band gap of the material and the photon energy. Absorption of photons with energies equal to or greater than the band gap of the semiconductor results in intrinsic absorption (interband absorption) process which is usually followed by an electronic transition across the band gap generating an electron-hole pair. The absorption coefficient for this absorption is typically large and varies greatly with wavelength. It can be about  $10^6 \text{ cm}^{-1}$  in the ultraviolet range and reach down to around  $1 \text{ cm}^{-1}$  just above the band gap energy. Absorption of photons with energies lower than the band-gap energy of the semiconductor results in different type of absorption. This type of absorption can result in electronic transitions within the allowed energy band or electronic transitions between localized impurity states and the conduction or valence band states. The absorption coefficient is usually a few orders of magnitude smaller for this type of absorption. [15]

Intrinsic optical absorption can be either a direct optical transition or an indirect optical transition as shown in Fig 2.3. A **direct optical transition** (DOT) occurs when the minimum of the conduction band is at the same point in **k**-space as the maximum of the valence band and the transition involves only absorption of a photon. An **indirect optical transition** (IOT) occurs when the minimum of the conduction band is at a different point in **k**-space from the maximum of the valence band. In this case the electron transition involves both absorption of a photon and a simultaneous absorption or emission of a phonon. The absorption coefficient is greater in DOT than in IOT and the difference can be about two orders of magnitude (i.e.  $10^4$  and  $10^2 \text{ cm}^{-1}$ ). The impact of different types of intrinsic optical excitation can be summarized in the following manner [15-17]

- Optical absorption occurs near the surface of materials with direct band gap, but for materials with indirect band gap there is a deeper penetration of light.
- For direct band gap materials, the magnitude of the intrinsic photoconductivity depends critically on the surface lifetime; the surface lifetime is much less important in indirect materials.
- Direct band gap materials have a higher intrinsic luminescence efficiency associated with a recombination of electrons and holes with emission of photons because of a shorter value of radiative recombination lifetime; indirect materials have lower intrinsic luminescence efficiency, since the longer lifetime for radiative recombination allows competing processes for non-radiative recombination to become important. Direct band gap excitation has much shorter lifetime than indirect.

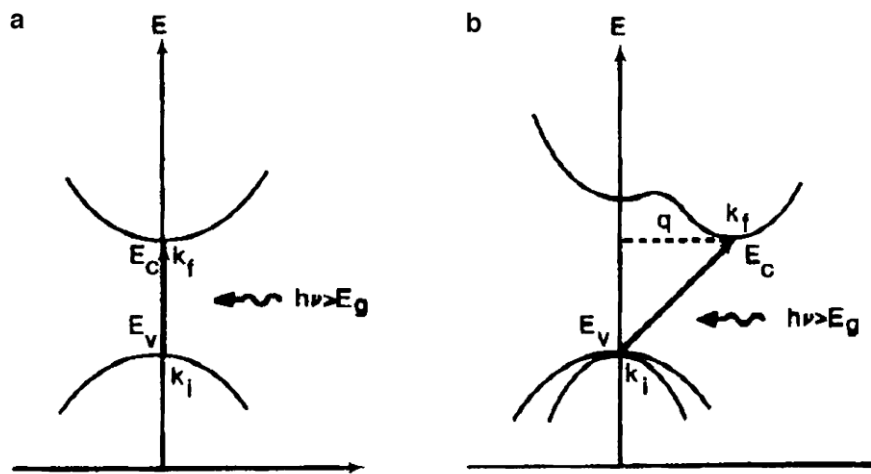


**Fig 2.3** Intrinsic a) direct absorption and b) indirect absorption. The band gap of a material is equal to the difference between the energy of the conduction band,  $E_c$ , and the valance band  $E_v$ . [15]

Equation (4) can be rewritten as [18]

$$\sigma = q(n_0\mu_{n0} + p_0\mu_{p0}) \quad (5)$$

If absorbed photons with energies equal or higher than the band gap of the semiconductor lead to generation of excess electron-hole pairs,  $\Delta n$  and  $\Delta p$ , then the charge carrier concentrations are increased to  $n = n_0 + \Delta n$  and  $p = p_0 + \Delta p$ . Photoexcitation may also change the carrier mobility,  $\Delta\mu$ . Considering only one type of carriers for simplicity, the conductivity under illumination is

$$\sigma_L = \sigma_0 + \Delta\sigma = q(n_0 + \Delta n)(\mu_0 + \Delta\mu) \quad (6)$$

And the net change in electrical conductivity in light

$$\Delta\sigma = q\mu_0\Delta n + (n_0 + \Delta n)q\Delta\mu \quad (7)$$

## 2.4 Hall effect

Hall effect measurement can be used to evaluate the electronic transport properties in a material. If a material is placed in a magnetic field and while a current is driven in a direction perpendicular to the magnetic field the charge carriers will be deflected in a direction normal to both the magnetic field and the current direction. The measurement configuration is shown in Fig 2.4.

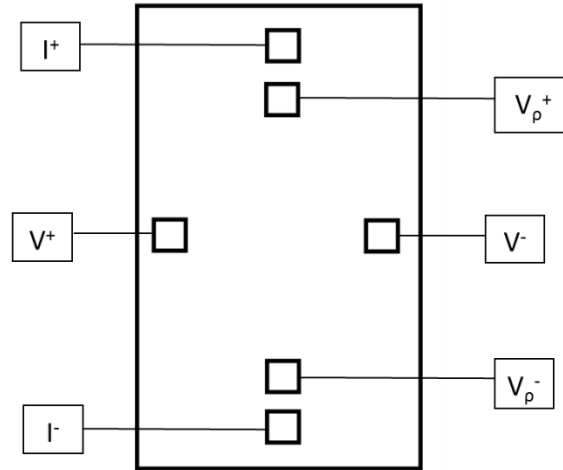


**Fig 2.4** Schematic drawing of the measurement configuration. Magnetic field is applied in or out of plane. Current flows from  $I^+$  to  $I^-$ , Hall voltage is measured between  $V^+$  and  $V^-$  and ohmic voltage is measured between  $V_p^+$  and  $V_p^-$ . Aluminum electrodes are connected from the instrument to the sample.

The buildup of charges on one side of the material will generate a potential that can be measured between  $V^+$  and  $V^-$  and is known as the Hall voltage. It can be written as [19]

$$V_H = \frac{IB}{end} \quad (8)$$

where  $V_H$  is the Hall voltage,  $I$  is the electrical current,  $B$  is the magnetic field,  $n$  is the carrier concentration,  $e$  is the elementary charge and  $d$  is the sample thickness.

The Hall coefficient is defined as [20]

$$R_H = \frac{E_y}{j_x B} = -\frac{1}{ne} \quad (9)$$

where  $E_y$  is the induced electric field and  $j_x$  is the current density. Since  $e$  is positive by definition the Hall coefficient becomes negative for free electrons. The Hall coefficient can be used to determine the carrier concentration in a material as well as the type of conductivity. An experimental setup was designed to perform the Hall effect measurement under illumination described in chapter 3.2.

### 3. Materials and methods

Thermoelectric and electronic transport properties of selected semi-conductors with various band gaps were measured in dark and under illumination. The emission spectra of the light sources can be found in the Appendix.

#### 3.1 Thermoelectric measurements

An ULVAC-RIKO ZEM-3 instrument was used to simultaneously measure the Seebeck coefficient and electrical resistivity of the samples. A schematic of the measurement setup is shown in Fig 3.1.

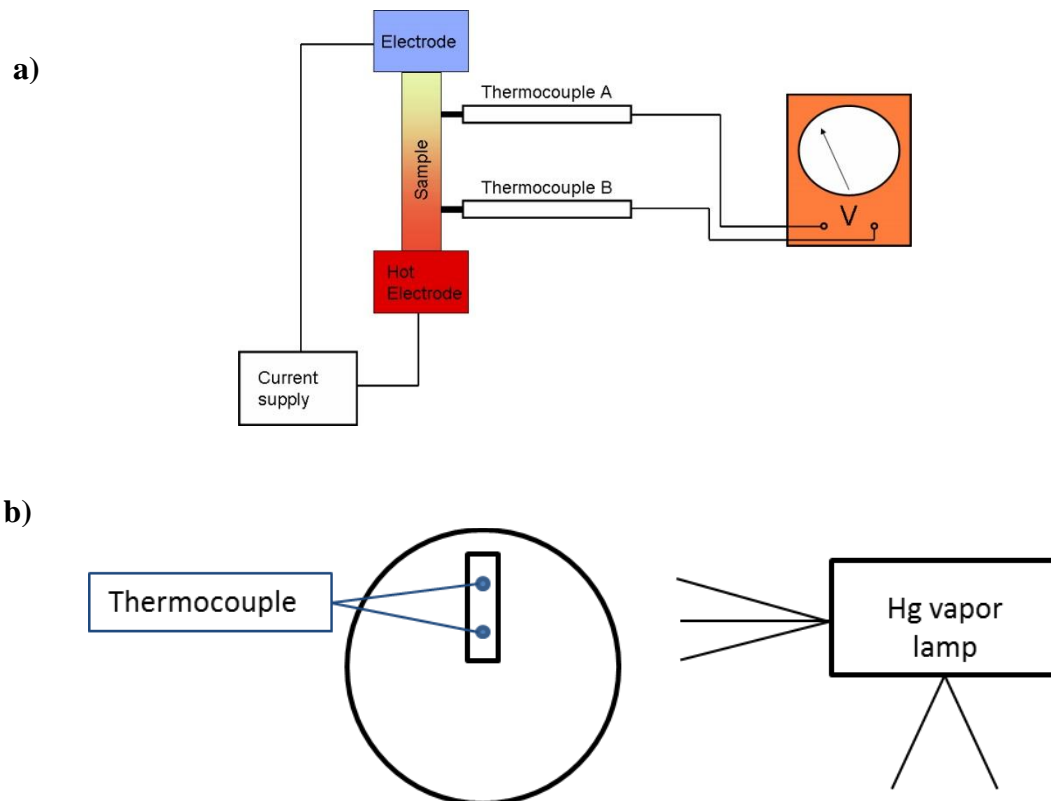


**Fig 3.1** a) Schematic of the ZEM-3 instrument used for measurements of the TE properties [21]. b) A mercury vapor lamp was positioned normal to the sample position in the ZEM-3 instrument.

A sample is clamped between two electrodes and a thermal gradient is applied through the hot electrode. The temperature difference and the generated potential difference, which are used to determine the Seebeck coefficient, were measured by the thermocouples. The measurements were performed at room temperature with temperature gradients of 10, 20 and 30°C between the two electrodes. A four point probe method is used to measure the resistivity, where a current is driven through the sample by the electrodes and a potential difference is measured by the thermocouples. All measurements were performed in low pressure helium environment, inside a quartz tube. A mercury vapor lamp with tunable light intensity was used as a light source and was positioned normal to the sample position, outside the sample chamber.

### 3.2 Hall effect measurements

Hall effect measurements were conducted in an instrument from Quantum Design, physical properties measuring system (PPMS). The experimental setup is shown in Fig 3.2.

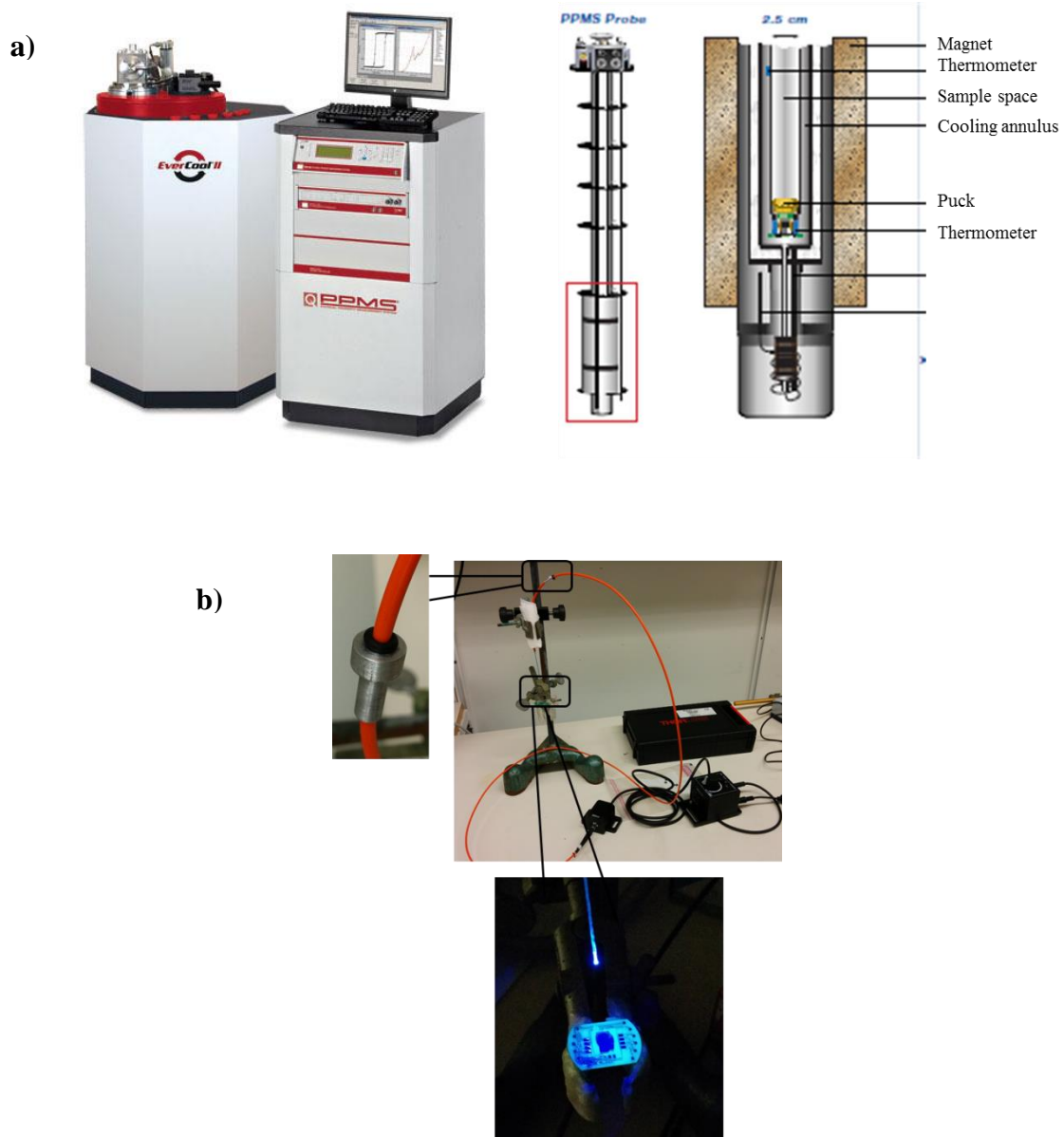


**Fig 3.2** a) An image of the PPMS. The probe is placed in a compartment with a tunable magnetic field. A sample is mounted on the puck and the sample chamber is under vacuum during measurements. b) An optical fiber was positioned 2-3 cm above the sample. An aluminum plug and a rubber O-ring was used to seal the opening where the fiber was introduced on top of the PPMS probe. A LED lamp with tunable light intensity was used as a light source and connected to the other end of the fiber.

A PPMS probe is inserted in a compartment with a tunable magnetic field. In the sample chamber of the probe there is a puck where a sample is mounted. During measurements the sample chamber is under vacuum. An experimental configuration was designed to enable

illumination of the samples during measurements. An optical fiber was positioned 2-3 cm above the sample, or till the light illuminates the whole sample. The fiber was thread through the PPMS probe and to hold vacuum in the sample chamber a metal plug and a rubber O-ring were used to seal the opening on top of the PPMS probe where the fiber is inserted. The fiber is connected to a 385 nm (3,2 eV) LED lamp with tunable light intensity. Hall voltage was measured at magnetic fields from -5 to +5 Tesla (in and out of plane) in dark and under illumination.

## 4. Results and discussion

The results are divided into sections where the results for each material are presented separately and the results are summarized and discussed in section 4.4.

### 4.1 Magnesium silicide

The TE properties of magnesium silicide were measured in dark and under illumination of a mercury vapor lamp. As shown in Fig 4.1, the illumination did not have a statistical significant impact on the electrical resistivity or the Seebeck coefficient. The Seebeck coefficient showed a negative value, which suggests that it is an n-type semi-conductor. Theoretical calculations have predicted the band gap of magnesium silicide to be around 0,3 eV [22], which is lower than the energy of the photons from the mercury vapor lamp and would allow an electronic transition from the valance band across the band gap to generate an electron-hole pair.  $Mg_2Si$  has a large light absorption coefficient [23] and in the light penetrated region is expected to reach about 10 nm into the material which is less than 0,001% of the thickness of the sample (1,3 mm). Several attempts were made to decrease the thickness of the material to boost the overall effect of the light but the material fell apart when it was mounted in the instrument.

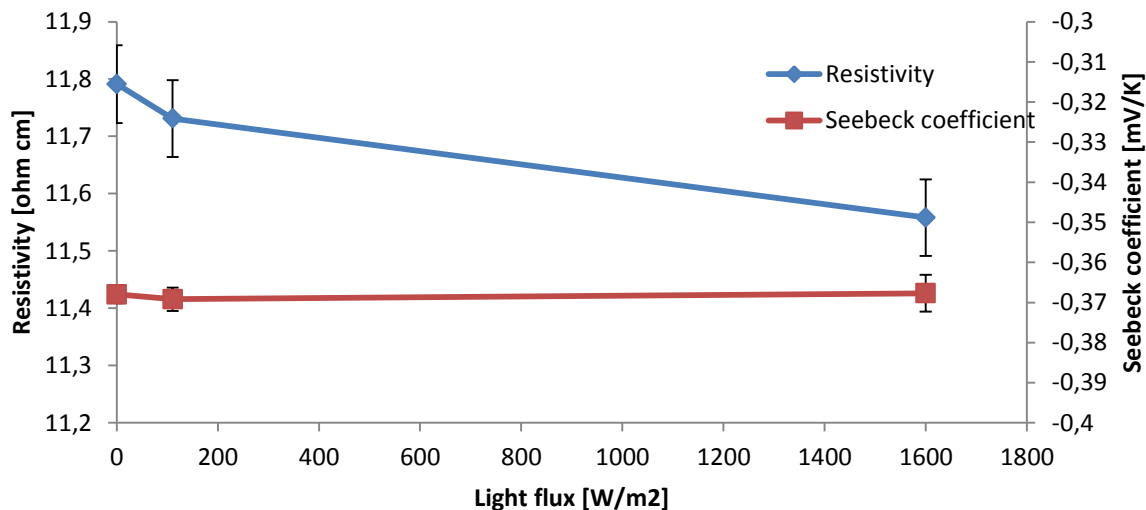


**Fig 4.1** Electrical resistivity and the Seebeck coefficient of  $Mg_2Si$  measured at 32°C in dark and with varying light intensity, measured in ZEM-3.

#### 4.1.1 Hall effect

Hall effect measurements were performed to evaluate the effect of light on the charge carrier concentration in the material. The light source is a 385 nm LED lamp and the experimental setup is described in detail in chapter **Error! Reference source not found.** Fig 4.2 shows the Hall voltage measured in dark and under light. The results confirm that the material is an n-type material and the carrier concentration is measured to  $1,4 \cdot 10^{17} \text{ cm}^{-3}$ , both in dark and under illumination. The LED lamp has about 3% of the photon energy that is offered with the mercury lamp which might explain why the carrier concentration was not affected.

The geometry of the sample is important, specifically the thickness of the sample. To maximize the impact of light on the materials electronic properties the sample thickness should be as close to the absorption layer as possible. The sample thickness was 150  $\mu\text{m}$  while it was 1300  $\mu\text{m}$  in the TE measurements.

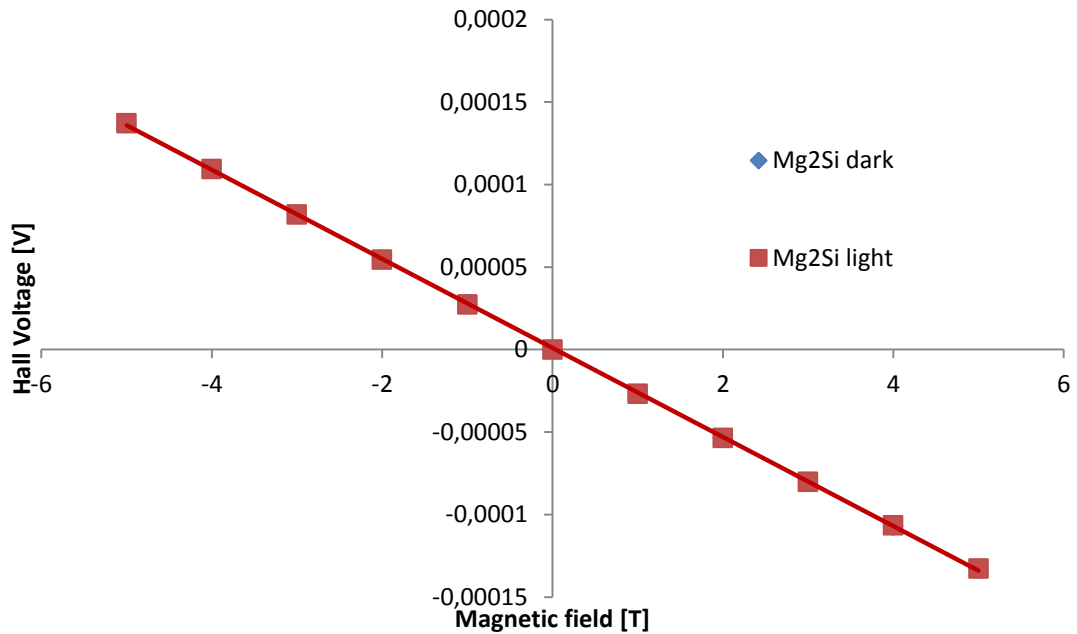
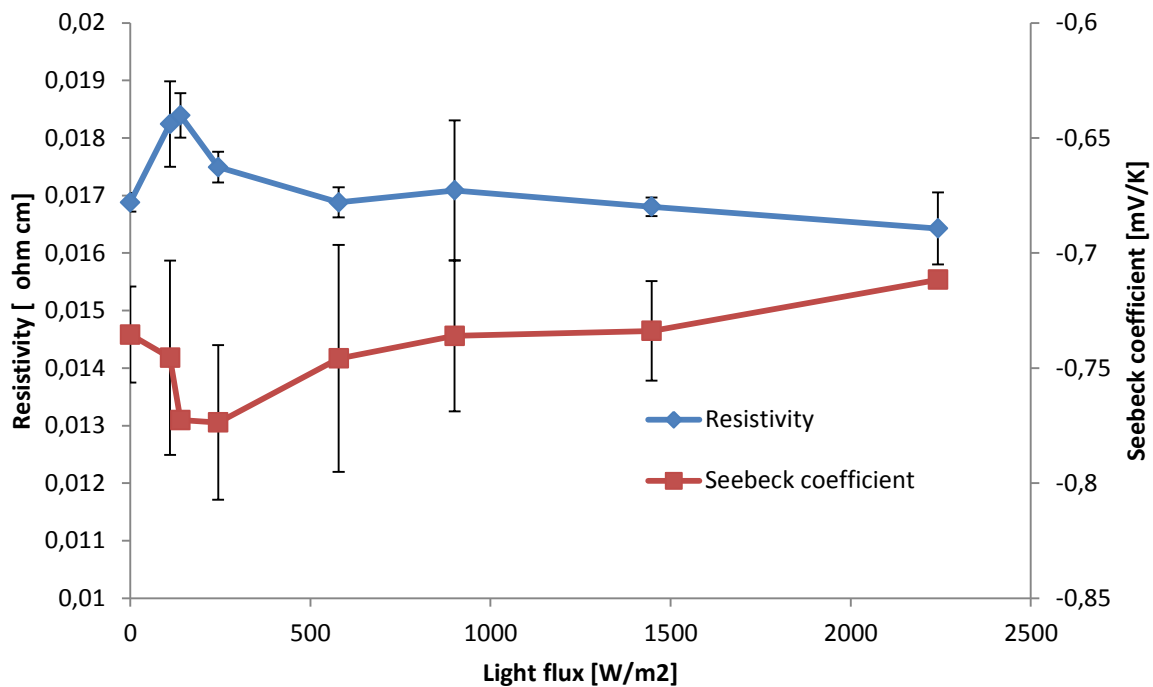


Fig 4.2 Hall voltage measurements in dark and with maximum light intensity.

## 4.2 Silicon

The TE properties of a silicon wafer were measured in dark and under illumination and are shown in Fig 4.3. A negative Seebeck coefficient shows that the material is n-type. The resistivity in dark was measured to 0,017 ohm cm, which suggests a carrier concentration of  $1,7 \cdot 10^{18}$  [24]. An increase in the resistivity is observed at intensities below 1000  $\text{W}/\text{m}^2$ , whereas above that it is slightly decreased. A negative photoconductivity is known to occur and is usually explained by a series of steps, including extrinsic excitation where the net effect is an electron transfer from the conduction band to a sensitizing center that was empty in the dark. This is commonly related to excitation with photons with energy lower than the band gap of the material [16]. Increase in electrical resistivity typically means a rise in the absolute Seebeck coefficient and that tendency is observed here. The absolute Seebeck coefficient was increased at light flux below  $1000 \text{W}/\text{m}^2$ , reaching a maximum at  $140 \text{W}/\text{m}^2$ . The maximum induced increase in resistivity is 8% and a 5% increase in the absolute Seebeck coefficient is observed.



**Fig 4.3** Electrical resistivity and the Seebeck coefficient of a silicon wafer measured at 40°C in dark and with varying light intensity, measured in ZEM-3.

Similar results were published on a p-type silicon, an initial increase in the Seebeck coefficient and resistivity at lower intensities and then decrease at higher intensities. It was suggested that a difference in surface resistivity compared to the bulk resistivity of the sample produces two different thermoelectric voltages, which are affected differently by illumination [25]. However, it is worth mentioning that these results were debated by part of the same group later where, after repeating the measurements on the same samples, they conclude: “apparently anomalous photothermoelectric effect in p-type silicon is not a genuine physical effect of interest, but must have arisen from the particular sample treatment or measurement technique used in the earlier work” [26]. There are studies that have shown negative photoconductivity of different types of n-type silicon [27-29].

#### 4.2.1 Hall effect

Hall effect measurements were performed to evaluate the effect of light on the charge carrier concentration in the material. Fig 4.4 shows the Hall voltage measured in dark and under light. The results confirm that the material is an n-type material and the carrier concentration is measured to  $1,5 \cdot 10^{18} \text{ cm}^{-3}$  and is not affected by the light illumination. The sample thickness is 230  $\mu\text{m}$  and the optical absorption depth is 35 nm at the wavelength provided by the LED lamp [30].

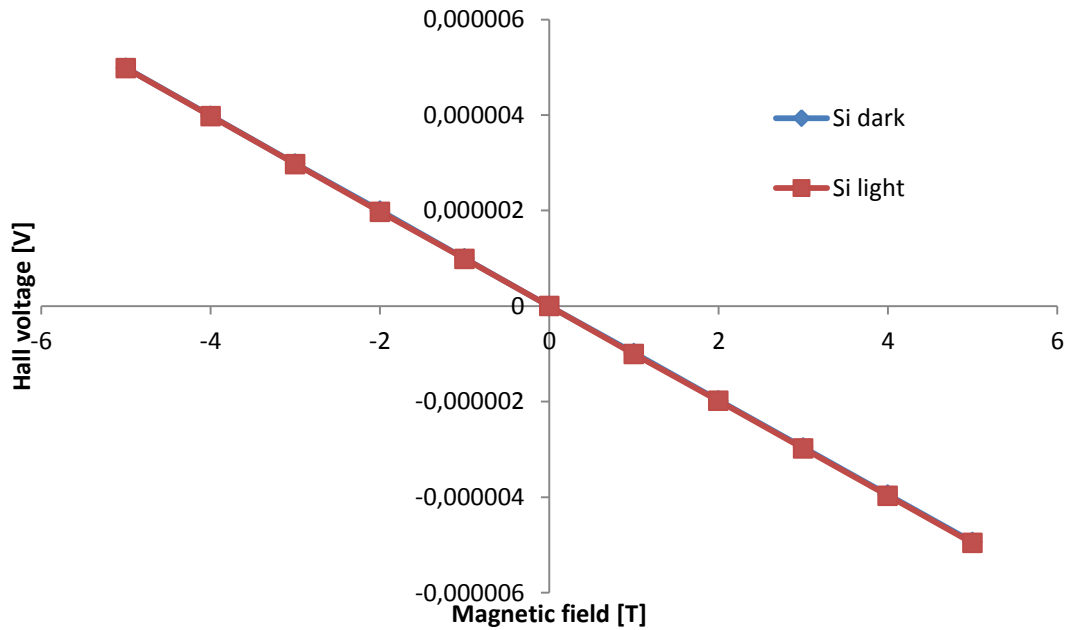


**Fig 4.4** Hall voltage measured on a silicon wafer at magnetic fields from -5 to +5 T, in dark and under illumination of a 385 nm LED lamp.

### 4.3 Titanium dioxide rutile

The TE properties of a single crystal  $\text{TiO}_2$  rutile were measured in dark and under illumination and the results are shown in Fig 4.5. The negative value of the Seebeck coefficient indicates that electrons are the majority charge carriers in the sample, i.e. it is a n-type semi-conductor. The resistivity was measured to 52 ohm cm in dark and is decreased by 6% with light flux of  $900 \text{ W/m}^2$ . A 5% decrease in the absolute Seebeck coefficient is observed at the same light flux. A slight increase in resistivity is detected at  $250 \text{ W/m}^2$  and also the resistivity is increased at higher intensity compared to the minimum values. One conceivable explanation is that at high light flux the number of charge carriers becomes so large that it lowers the mobility and consequently the conductivity of the material.

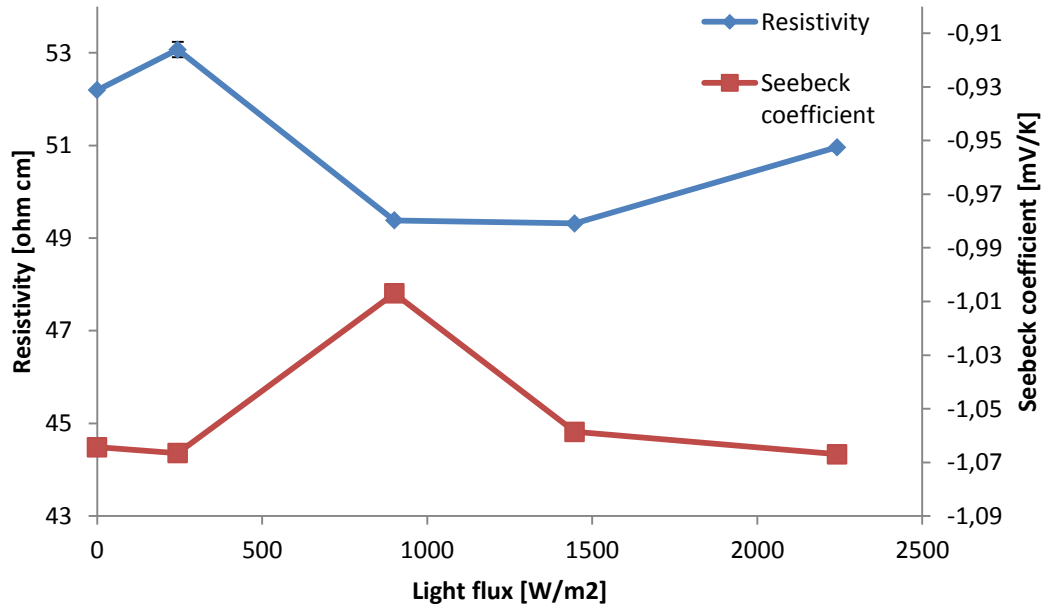
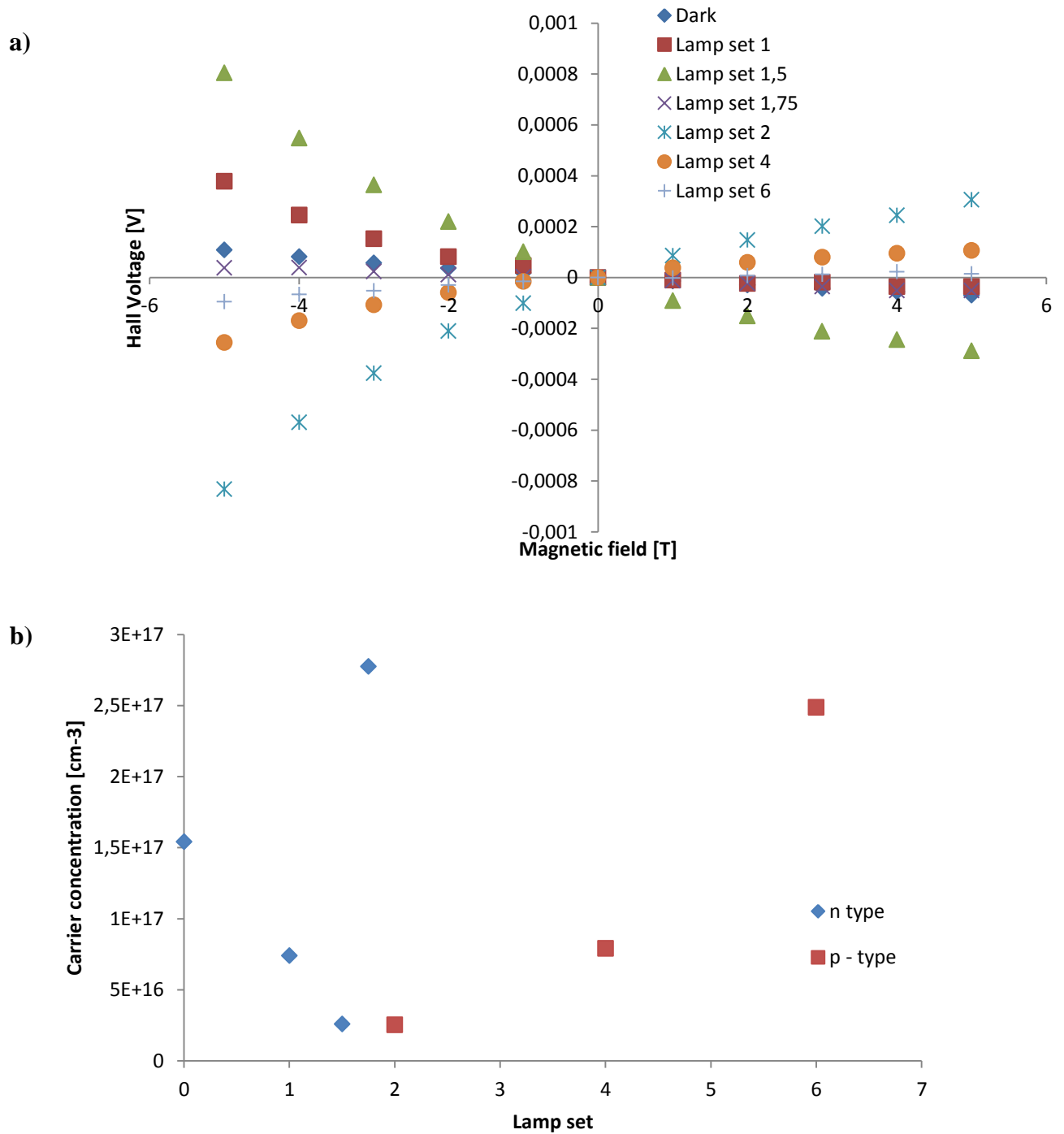


Fig 4.5 Electrical resistivity and the Seebeck coefficient of a single crystal rutile measured at 43°C in dark and with varying light intensity, measured in ZEM-3.

### 4.3.1 Hall effect

Hall effect measurements were carried out on the same rutile sample. The sample thickness was minimized to enlarge the influence of the light flux on the bulk electronic transport properties. The sample was attached to a glass slide and polished with silicon carbide paper to approximately 200µm. The absorption layer is estimated to be about 25 µm [31].

Hall effect measurements were carried out in dark and at 6 different light intensities of the LED lamp. As seen in Fig 4.6 the light illumination has a large effect on the measured Hall voltage. A negative slope in dark confirms that the sample is a n-type material and the carrier concentration is measured to  $1,5 \cdot 10^{17} \text{ cm}^{-3}$ . At lower intensities the carrier concentration is decreased but when the intensity is increased to 3,6 W/m<sup>2</sup> (Lamp set 2) the slope of the curve becomes positive, indicating a transition from n- to p-type conduction, and with further increased light flux the material shows still a p-type conduction with a higher carrier concentration. One point stands out, at lamp set 1,75 (2,6 W/m<sup>2</sup>) the n-type carrier concentration was measured higher than in dark. It remains unclear what causes this, but the point is close to where the switch to p-type is observed which could possibly explain this behavior.



**Fig 4.6** Hall effect measurements were performed to evaluate how the electron transport properties of the material are affected by light flux. a) Hall voltage measurements on a single crystal rutile sample, in dark and with varying light intensities of 385 nm LED lamp. The lamp setting is ordered from the lowest to the highest intensity. b) The relationship between carrier concentration and lamp setting. A negative carrier concentration represents a n-type conductivity and a positive represents a p-type conductivity.

Titanium dioxide rutile is a wide band gap semi-conductor with a low temperature optical direct band gap of 3,0 eV [32]. An electron self-trapping below the conduction band has been reported both by theoretical calculations [33] and by EPR measurements [34]. Trapped

electrons have low mobility and do not contribute to the electrical conductivity of a material. A proposed mechanism is shown in Fig 4.7.

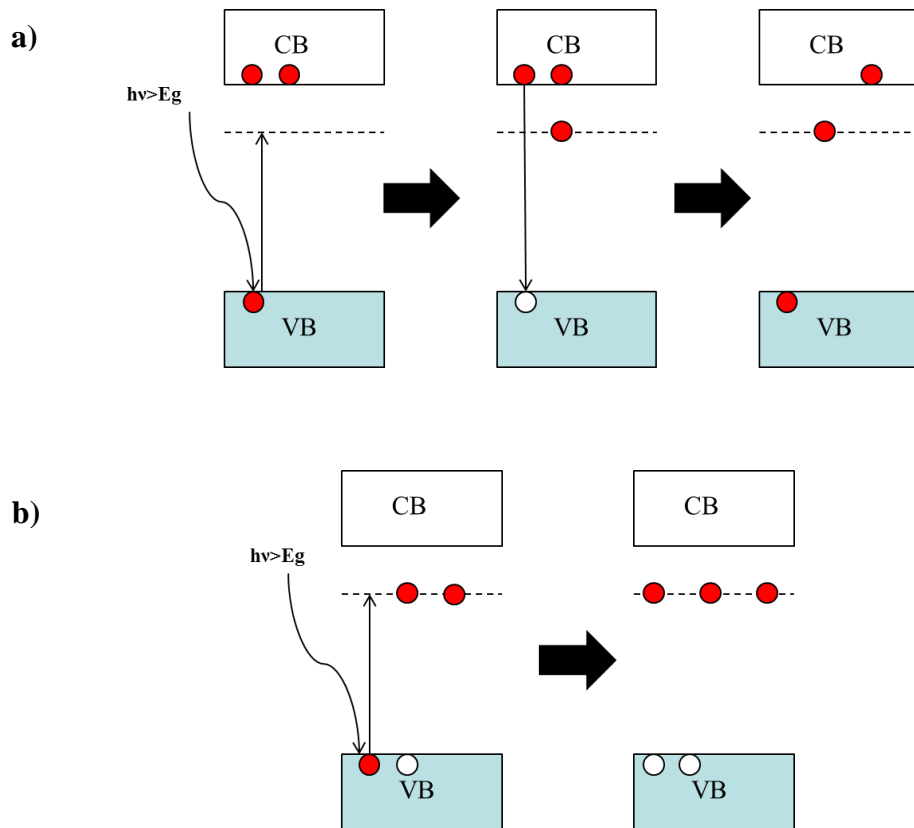


**Fig 4.7** Electron is excited from the valance band (VB) to the trapped state (dotted line), generating a hole in the VB. **a)** An electron drops down from the conduction band (CB) and the net change is a decrease in electrons in the CB. **b)** an electron is excited from the VB to the trapped state.

Photons excite electrons from the valance band (VB) to the trapped state, generating hole in the VB which recombines with an electron from the conduction band (CB). The net change is an electron drop from the CB to the trapped state. If the photon flux is increased enough the CB will be emptied of free electrons. Electrons will be excited from the VB to the trapped state without any recombination and the hole concentration will be increased with increasing photon flux. Theoretical calculations have suggested that the electrons self-trapping arise from  $Ti^{4+}/Ti^{3+}$  acceptor transitions near the donor impurity and  $TiO_2$  contains about  $3 \cdot 10^{20} \text{ cm}^{-3}$  oxygen vacancies [33] which suggests that the trapped state would be able to carry the electrons from the CB and still accept electrons from the VB at high intensities.

#### 4.4 Carrier concentration and TE properties

The electromagnetic radiation had a large impact on the electronic transport properties of  $TiO_2$  rutile while it did not have a measureable impact on single crystal silicon or  $Mg_2Si$ . Rutile has a much larger band gap than both  $Mg_2Si$  and Si and electron self-trapping level provides a possible mechanism for the observed switch from n- to p-type conduction. Another important factor is the absorption layer which is larger for  $TiO_2$  than the other materials.

No clear correlation was observed between the TE properties measurements and the carrier concentration measurements. A switch from n- to p- type conduction would have resulted in a positive Seebeck coefficient, which was not observed. A reason for this could be that the sample thickness was about 5 times greater when the sample was mounted in the ZEM-3 instrument compared to the PPMS. Another difference in the measurement condition is the applied temperature gradient in the material during the measurements of the TE properties. The temperature difference causes a build-up of charges, both holes and electrons, on the cold side. If an electron – hole pair is generated and both charge carriers diffuse to the same side of the material they will cancel each other out so no difference in electric potential will be observed. However, a current flowing through the material will drive the charge carriers in opposite direction and it is expected that a generated electron–hole pair would increase the electrical conductivity of the material. No clear evidence of this is observed in the measurements although the illumination seems to have some effect on the conductivity and the Seebeck coefficient of the measured materials.

## 5. Conclusion

Improving the efficiency of thermoelectric materials would increase their applicability in various fields where energy is wasted as heat. The carrier concentration has a great impact on the TE properties of a material. The carrier concentration in a semi-conductor is typically tuned with chemical doping, which requires synthesis a series of materials with different amounts of doping. Another way to tune the carrier concentration is to shine light onto the material. A photon can excite an electron from the valance band to the conduction band, generating an electron–hole pair.

The electromagnetic radiation had a large impact on the electronic transport properties of a single crystal  $\text{TiO}_2$  rutile while it did not have a measureable impact on single crystal silicon or  $\text{Mg}_2\text{Si}$ . An unexpected, and to my knowledge not previously recorded, switch from n– to p–type conduction was observed on  $\text{TiO}_2$  with illumination. A decrease in free electron concentration was observed at low intensities, then a switch to p-type conduction at higher intensities followed with an increasing hole concentration when the light flux was further increased. A mechanism which includes self-trapping of electrons was proposed, which can explain the measured effect.

The light illumination had some effect on the TE properties of the materials, however there was no clear trend observed with varying light intensities.

The method of using electromagnetic radiation to find the optimum carrier concentration for TE materials may be useful but it has sample demands. It may be useful for thin film samples or where the light absorption layer has a measurable contribution to the overall values of the TE properties or the carrier concentration. The method might also have some limitation with regards to the band gap and band structure of the sample.

## Acknowledgements

I would like to thank Professor Anders Palmqvist for giving me the opportunity to work on this project and for all the encouragement and guidance during my work.

I would also like to express my gratitude to the following people:

Richard Heijl for all the support and guidance during my work on this project. I am thankful for all the time you made to help me out.

Björn Elgh for the fruitful discussions, for inspiring me when I needed inspiration and confusing me when I needed to get confused.

Alexey Kalabukhov for the help with the Hall effect measurements.

Kurt Löfgren for the help with building the experimental setups.

The people at TYK for the great atmosphere in the department. I would like to give special thanks to the people in the master thesis room for all the good times we had both in and outside the office. I also want to mention my group mates in the AP group for the rewarding discussions in the group meetings.

## References

1. Seebeck, T.J., *Ueber den magnetismus der galvenische kette*. Abh. K. Akad. Wiss. Berlin, 1821. **289**.
2. Seebeck, T.J., *Magnetische polarisation der metalle und erze durch temperatur-differenz*. Abh. K. Akad. Wiss. Berlin, 1823. **265**.
3. Seebeck, T.J., *Ann. Phys.*, 1826. **83**.
4. Seebeck, T.J., *Platinatiegel auf ihr chemische reinheit durch thermomagnetismus zu prufen*. Schweigger's J. Phys., 1826. **46**.
5. Peltier, J.C., *Ann. Chim. Phys.*, 1834. **56**: p. 371.
6. Prasad, M., *Refrigeration and Air Conditioning*. 2003: New Age International.
7. Thomson, W., *On a mechanical theory of thermoelectric currents*. Proceedings of the Royal Society of Edinburgh, 1851. **91**: p. 1851.
8. Altenkirch, E., *Uber den Nutzeffekt der Thermosaule*. Physikalische Zeitschrift, 1909. **10**: p. 560.
9. Altenkirch, E., *Elektrothermische Kälteerzeugung und reversible elektrische Heizung*. Physikalische Zeitschrift, 1911. **12**: p. 920-924.
10. Dresselhaus, M.S., et al., *New Directions for Low-Dimensional Thermoelectric Materials*. *Advanced Materials*, 2007. **19**(8): p. 1043-1053.
11. Snyder, G.J. and E.S. Toberer, *Complex thermoelectric materials*. *Nat Mater*, 2008. **7**(2): p. 105-114.
12. Okazaki, R., et al., *Photo-Seebeck Effect in ZnO*. *Journal of the Physical Society of Japan*, 2012. **81**(11): p. 114722.
13. Snyder, J. *Thermoelectrics, Caltech Materials Science* - <http://thermoelectrics.caltech.edu/thermoelectrics/index.html>. **2014**.
14. Vaqueiro, P. and A.V. Powell, *Recent developments in nanostructured materials for high-performance thermoelectrics*. *Journal of Materials Chemistry*, 2010. **20**(43): p. 9577-9584.
15. Li, S.S., *Semiconductor Physical Electronics*. Microdevices. 2006: Springer New York.
16. Bube, R.H., *Photoelectronic properties of semiconductors*. 1992.
17. Kittel, C., *Introduction to Solid State Physics*. 8th ed. 2005: John Wiley & Sons, Inc.
18. Bube, R.H., *Photoelectronic Properties of Semiconductors*. 1992: p. 18-21.
19. Thurber, W.R. *Hall effect measurements* - <http://www.nist.gov/pml/div683/hall.cfm>. 2008 November 21, 2011 [cited 2014].
20. Kittel, C., *Introduction to Solid State Physics*. 2005: John Wiley and Sons. 154.
21. GUILMEAU, E. *High temperature resistivity and Seebeck measurement* - <http://www-crismat.ensicaen.fr/spip.php?article319>. 2008 [cited 2014 August 27].
22. Imai, Y. and A. Watanabe, *Energetics of alkaline-earth metal silicides calculated using a first-principle pseudopotential method*. *Intermetallics*, 2002. **10**(4): p. 333-341.
23. Kato, T., Y. Sago, and H. Fujiwara, *Optoelectronic properties of Mg<sub>2</sub>Si semiconducting layers with high absorption coefficients*. *Journal of Applied Physics*, 2011. **110**(6): p. -.
24. Filliben, J.J., et al., *The Relationship between resistivity and dopant density for phosphorus- and boron-doped silicon*. *Semiconductor measurement technology*. 1981, Washington, D.C.: U.S. Dept. of Commerce, National Bureau of Standards : For sale by the Supt. of Docs., U.S. G.P.O. v, 47 p.
25. Harper, J.G., H.E. Matthews, and R.H. Bube, *Photothermoelectric Effects in Semiconductors: n- and p-Type Silicon*. *Journal of Applied Physics*, 1970. **41**(2): p. 765-770.

26. Kwok, H. and R.H. Bube, *Another Look at the Anomalous Photothermoelectric Effect in p-Type Silicon*. Journal of Applied Physics, 1970. **41**(12): p. 5026-5027.
27. Penchina, C.M., J.S. Moore, and N. Holonyak, *Energy Levels and Negative Photoconductivity in Cobalt-Doped Silicon*. Physical Review, 1966. **143**(2): p. 634-636.
28. Kurosu, T., et al., *Transient negative photoconductivity in silicon doped with gold*. Applied Physics A, 1987. **43**(3): p. 205-208.
29. Jiang, C.-S. and S. Hasegawa, *Photoconductivity of the Si(111)-7×7 and 3×3-Ag surfaces*. Surface Science, 1999. **427–428**(0): p. 239-244.
30. Martin, A.G. and M.J. Keevers, *Optical properties of intrinsic silicon at 300 K*. Progress in Photovoltaics: Research and Applications, 1995. **3**.
31. Pascual, J., J. Camassel, and H. Mathieu, *Fine structure in the intrinsic absorption edge of TiO<sub>2</sub>*. Physical Review B, 1978. **18**(10): p. 5606-5614.
32. Amtout, A. and R. Leonelli, *Optical properties of rutile near its fundamental band gap*. Physical Review B, 1995. **51**(11): p. 6842-6851.
33. Deák, P., B. Aradi, and T. Frauenheim, *Quantitative theory of the oxygen vacancy and carrier self-trapping in bulk TiO<sub>2</sub>*. Physical Review B, 2012. **86**(19): p. 195206.
34. Macdonald, I.R., et al., *EPR studies of electron and hole trapping in titania photocatalysts*. Catalysis Today, 2012. **182**(1): p. 39-45.

## Appendix

The emission spectra were analyzed with Ocean Optic USB2000+ spectrometer. A mercury vapor lamp was used to illuminate the samples during the ZEM-3 measurements. The thermoelectric properties, Seebeck coefficient and the resistivity, were measured in dark and under illumination with various intensities.

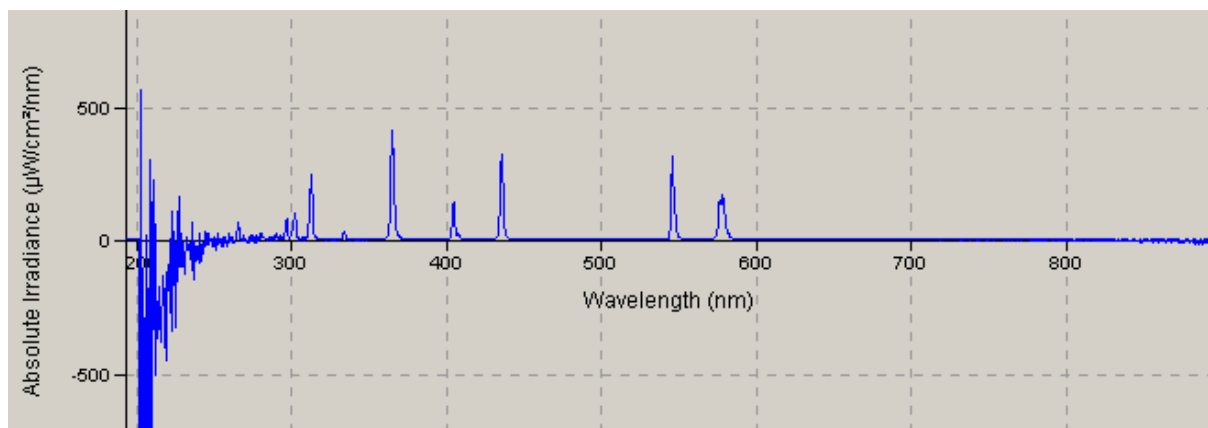
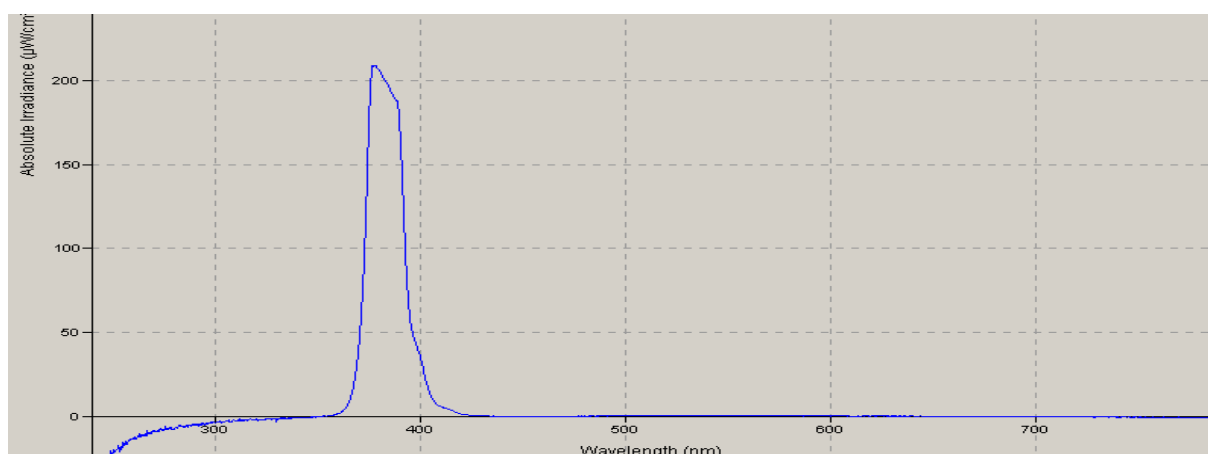


**Figure** Several peaks are observed at wavelengths between 300 and 600 nm. Peaks below 250 nm are regarded as noise from the spectrometer and can be neglected.

The mercury lamp emits light at wavelengths between about 300-600nm which corresponds to about 4,1 to 2,1 eV in photon energy, respectively. The photon power onto the samples was measured by integrating the spectra from 250-800 nm.

During the Hall effect measurements a LED 385 nm lamp was used. The maximum photon power was measured to be about 3% of the maximum of the mercury vapor lamp during TE measurements.



The materials that have been analyzed are listed in table 1 below.

**Table 1. Materials that were investigated**

Material	Bandgap	Carrier concentration (cm <sup>-3</sup> )	Sample geometry (height x width x depth) (mm)
n-Bi <sub>2</sub> Te <sub>3</sub> *	0,15	7,3x10 <sup>20</sup> (m. by Ma Yi.)	10x2,85x0,0003
Mg <sub>2</sub> Si	0,3	1,4x10 <sup>17</sup>	9,6x3,053x1,384
n-Silicon wafer	1,1	1,5x10 <sup>18</sup>	10x3,885x0,530
TiO <sub>2</sub> Rutile	3,0	1,5x10 <sup>17</sup>	7,073x7,044x1,037

\*Light source at 30° angle to sample.

The materials have bandgaps from 0,15-3,0 eV and varying carrier concentrations.